The Journal of International Advanced Otology

J Int Adv Otol 2023; 19(5): 368-375 • DOI: 10.5152/iao.2023.23695

Original Article

Calculation of the Faradaic Impedance of the Electrode–Tissue Interface Improves Prediction of Behavioral T/C Levels in Cochlear Implant Patients

Andrzej Zarowski, Marc Leblans, Andrzej Molisz, Fergio Sismono, Joost van Dinther, F. Erwin Offeciers

European Institute for Otorhinolaryngology, Sint-Augustinus Hospital, Antwerp, Belgium

ORCID iDs of the authors: A.Z. 0000-0002-8811-0655, M.L. 0000-0002-9390-5962, A.M. 0000-0003-3662-1581, F.S. 0000-0002-4611-8632, J.v.D. 0000-0002-5275-7852, F.E.O. 0000-0002-3181-9823.

Cite this article as: Zarowski A, Leblans M, Molisz A, Sismono F, van Dinther J, Offeciers FE. Calculation of the faradaic impedance of the electrode–tissue interface improves prediction of behavioral T/C levels in cochlear implant patients. *J Int Adv Otol.* 2023;19(5):368-375.

BACKGROUND: Fitting of cochlear implants is a labor-intensive process, and therefore automated fitting procedures are being sought. The objective of this study was to evaluate if decomposition of the complex impedance of the electrode–tissue interface could provide additional parameters that show improved correlation with the behavioral T/C levels.

METHODS: A new method for decomposing the complex impedance of the electrode–tissue interface was developed and tested in 18 patients in a prospective study in a tertiary otologic referral center.

RESULTS: The averaged near-field Faradaic resistance (R_F) calculated in study subjects shows a very strong correlation ($R^2 = 0.80$) with the behavioral C levels and can be used for automated fitting in most patients. The standard deviation for the T levels and the C levels calculated for each of the electrode contacts in all study subjects is in the range of 10-15 CL and 15-20 CL, respectively. These higher values of the standard deviations are caused by a few outliers who require that additional parameters have to be added to the metric equation, allowing for the automated prediction of the T/C levels.

CONCLUSION: A new method for deriving information from the electrode impedance measurements shows excellent correlation of the Faradaic resistance with the behavioral T/C levels in most patients and can be very useful for fitting cochlear implants based on objective measures. Since some patients still show discrepancies between the predicted T/C levels based on the R_F calculation, additional parameters have to be added to the metric equation, allowing for automated prediction of the T/C levels.

KEYWORDS: Cochlear implants, Faradaic, impedance, corresponding circuit, behavioral, T/C level

INTRODUCTION

Cochlear implants (CIs) have become very successful in the treatment of hearing loss and deafness, with 736 900 patients implanted worldwide by 2019 (https://www.nidcd.nih.gov/sites/default/files/Documents/cochlear-implants.pdf).

In order to make cochlear implants work in an optimal way, the stimulation parameters for each of the stimulating electrode contacts have to be individually adjusted in each patient. This process of defining the stimulation parameters is called implant fitting. In particular, the stimulation currents corresponding to the sensation thresholds (T levels) and to the levels of comfortable hearing (C levels) have to be defined. The T/C levels are the basic fitting parameters of a cochlear implant.

The behavioral measurement of the T/C levels for each electrode contact is a labor-intensive process that has to be regularly repeated in the postoperative period due to significant changes in the electrophysiological parameters over time after implantation researchers researchers.[1] This, together with the continuously increasing number of implanted patients, creates a big burden to the cochlear implant centers and results in shortages of audiological resources. Therefore, solutions for automated and/or streamlined

The first two authors contributed equally to this manuscript.

Corresponding author: Andrzej Zarowski, e-mail: andrzej.zarowski@me.com

Received: March 09, 2023 • **Accepted:** September 01, 2023 • **Publication Date:** September 29, 2023
Available online at www.advancedotology.org

fitting procedures have been sought. These fitting procedures are based mostly on electrophysiological measures such as electrically evoked compound action potentials (ECAP), electrically evoked auditory brainstem responses (EABR), or electrically evoked stapedius reflex thresholds (ESRT). However, all electrophysiological measures (ECAP, EABR, and ESRT) show very big variability and are unable to accurately predict the behavioral T/C levels. This has already been demonstrated by many researchers.[1-3]

Ourrecently published papers[4,5] show major improvements in the prediction of the behavioral T/C levels by analysis of impedances of the electrode contacts. These impedances show significant, strong negative correlations with the stabilized T/C levels at 4-6 months after implantation and are an important predictor for the behavioral T/C levels, especially for perimodiolar electrodes. In these electrodes, the electrode impedances can explain $R^2 = 28\%$-41% of the variability of the behavioral T/C levels.

The objective of this study was to evaluate if decomposition of the complex impedance of the electrode–tissue interface could provide parameters that show even better correlation with the behavioral T/C levels.

MATERIAL AND METHODS

Study Subjects

Eighteen adult patients (8 females and 10 males) have been included in the study. They were all recipients of the Nucleus Freedom, or CI500 series, implant manufactured by the Cochlear Ltd. Company and had at least 6 months of experience with the cochlear implant. The age of the patients was between 34 and 79 years at the moment of their inclusion in the study. Figure 1 shows the histogram of the age distribution. The demographic data of the study subjects are contained in Table 1. The study was performed at the European Institute for Otorhinolaryngology in Antwerp in Belgium and required a single visit during which the impedance data were collected and compared to the behavioral fitting maps derived from the Custom Sound database.

Ethical Considerations

This study was running under the Ethics Commission approval of CTC5585 “Innovation in Clinical Care for Users of a Nucleus Cochlear Implant”, obtained on January 9, 2015 from the Ethics Committee of the Sint Augustinus Hospital - Gasthuis Zusters Antwerpen (GZA). All study subjects signed the Patient Informed Consent (PIC) when entering the study.

MAIN POINTS

- Automatisation of cochlear implant fitting based on objective parameters could help in the management of increasing numbers of implanted patients and solve the problem of fitting in small children and non-cooperative patients.
- Faradaic resistance of the electrode–tissue interface calculated according to the method described in this paper shows excellent correlation with the behavioral T/C levels.
- This could improve the metric equation allowing for automated fitting of cochlear implants.

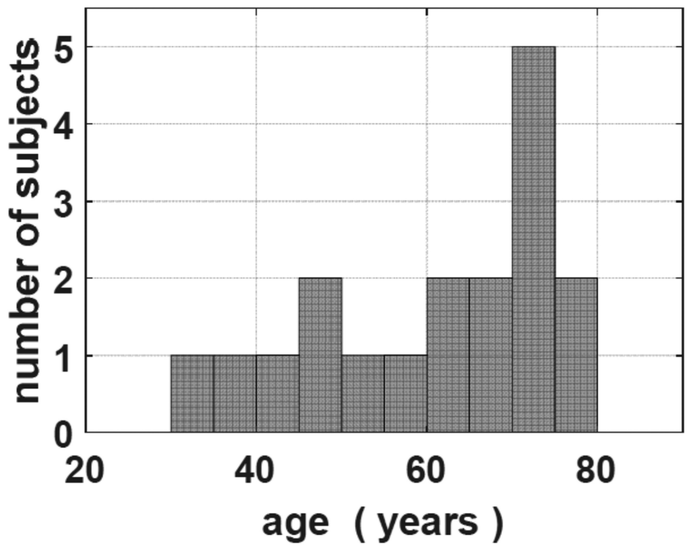

Figure 1. Age distribution of the 18 study subjects.

Statistical Analysis

Statistical analysis was performed with Statistica 13.3 (TIBCO Software Inc., Palo Alto, CA, USA). Pearson’s correlation coefficient was used throughout the report.

Description of the Impedance Model

The complex impedance of the electrode–tissue interface of the cochlear implant can be represented by the lump element model shown in Figure 2. It comprises an access resistance R_A corresponding to the near- and far-field tissue resistance in series with a parallel circuit of the double layer capacitor C_{DL} and a resistance R_F corresponding to the Faradaic processes occurring at the electrode–electrolyte interface (i.e., charge transfer or polarization resistance).[6,7]

In the equivalent circuit of Figure 2, one also recognizes the scheme of a simplified Randles cell.[8,9] Such a simplified Randles cell can serve as a starting point for other more complex models for representing the electrode–tissue interface.

An impedance model of the full interface comprising the electrode–tissue interface and the cochlear tissues, extracochlear reference electrodes, and DC blocking capacitor is provided in Figure 3.

The parameters of the impedance model characterize intrinsically different parts of the current path. As mentioned earlier, the model we use for the electrode–tissue interface comprises the double layer capacitance C_{DL}, the Faradaic resistance R_F, and the so-called bulk resistance R_B, which forms the middle-field part of the access resistance R_A. The parameters C_{DL} and R_F are related to the electrochemical processes in the closest vicinity of the electrode contact (near-field effects).[10] The double-layer capacitor C_{DL} is capable of storing electrical energy by means of the electrical double layer effect, which occurs at the interface between a conductive electrode of the intracochlear array of electrodes and the adjacent liquid electrolyte (i.e., the tissue between the electrode array and the other part of the cochlear implant). As already mentioned, the R_F corresponds to the Faradaic processes occurring at that interface. The bulk resistance R_B contains several components, such as the additional contribution to the impedance due to the current concentration near the electrode

Table 1. Demographic Data of the Study Subjects

Subject	Gender	Age at Study (Y)	Age at CI Surgery (Y)	Implant Type	Electrode	Ear	Etiology of Hearing Loss	Onset of Hearing Loss	Age at Onset of Hearing Loss (Y)	Duration of Hearing Loss (Y)
01	F	67	57	CI24RE	Contour Advance	R	Unknown	Progressive	32	25
02	M	34	23	CI24RE	Contour Advance	L	Meningitis	Sudden	10	13
03	M	71	61	CI24RE	Contour Advance	L	Familial	Progressive	Unknown	Unknown
04	F	38	29	CI24RE	Contour Advance	R	Unknown	Congenital	0	29
05	F	52	44	CI24RE	Contour Advance	L	Unknown	Congenital	0	44
06	F	60	57	CI24RE	Contour Advance	R	Trauma	Sudden	55	2
07	F	64	57	CI24RE	Contour Advance	L	Unknown	Progressive	48	10
08	M	71	65	CI24RE	Contour Advance	L	Ménière	Progressive	56	8
09	M	60	50	CI512	Contour Advance	R	Unknown	Progressive	10	40
10	F	79	68	CI24RE	Contour Advance	R	Unknown	Progressive	59	9
11	F	74	66	CI24RE	Contour Advance	R	Unknown	Progressive	40	30
12	M	71	69	CI512	Contour Advance	L	Unknown	Progressive	Since childhood	60
13	M	68	57	CI24RE	Contour Advance	L	Familial	Progressive	46	11
14	M	76	75	CI512	Contour Advance	R	Familial	Progressive	50	15
15	F	46	44	CI24RE	Contour Advance	R	Measles	Sudden	6	39
16	M	48	47	CI512	Contour Advance	L	Familial	Progressive	5	42
17	M	70	60	CI24RE	Contour Advance	L	Ménière	Sudden	56	4
18	M	40	39	CI512	Contour Advance	R	Ménière otosclerosis	Progressive	26	4

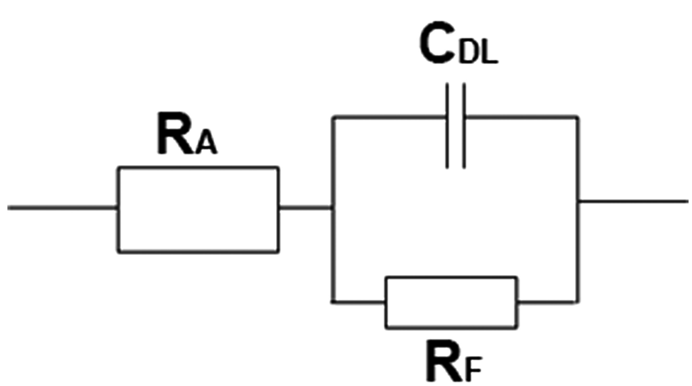

Figure 2. Model of the complex impedance of the electrode–tissue interface of the cochlear implant electrode contacts.

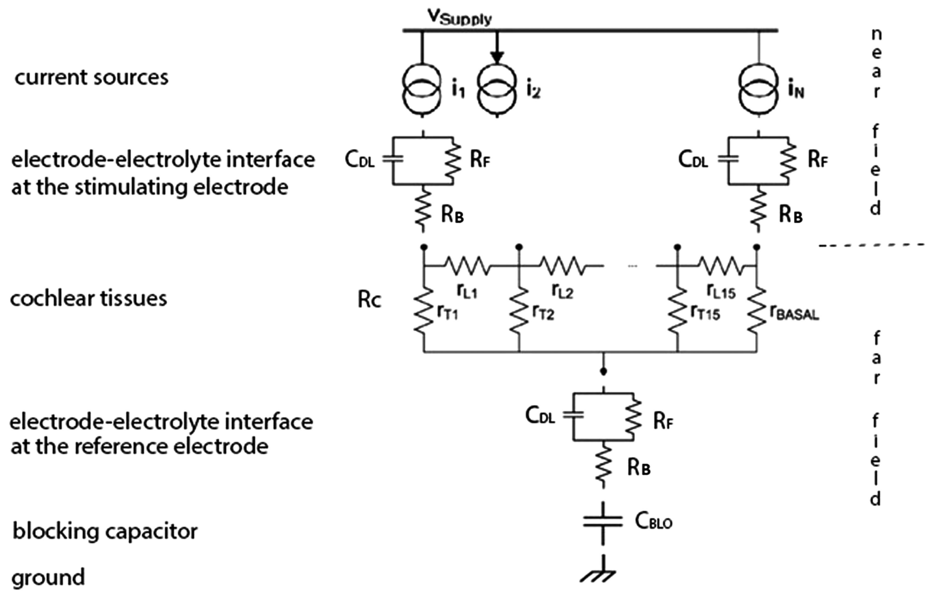

Figure 3. More complex model of impedance employing the near-, middle-, and far-field elements.

contact and tissue growth around it (these can be considered as the middle-field effect).[6,10,11] The effect of the tissue between the intracochlear electrodes and the extracochlear reference electrodes, i.e., the various transversal resistive components r_{Ti} and longitudinal components r_{Li} depicted in Figure 3, is lumped together into the single resistive component R_C (Figure 4), which represents the far-field component.[12] Note that the access resistance R_A of Figure 2 is equal to the sum of R_B and RC in Figure 3.

The capacitance between the extracochlear reference electrodes and the stimulation/recording circuitry (including the serial blocking capacitor between each individual current source and stimulation contact) is shown in Figures 3 and 4, denoted as C_{BLO}. The impedance parameters of the reference electrodes are pragmatically less important than the impedance parameters of the intracochlear electrodes due to their much larger dimensions.[13]

The parameters of the electrical circuit corresponding to the impedance of the electrode–electrolyte interface can be determined by applying the following approach. In some embodiments, rectangular biphasic pulses are generated between two chosen electrodes in the electrode array. In other embodiments, nonrectangular pulses can

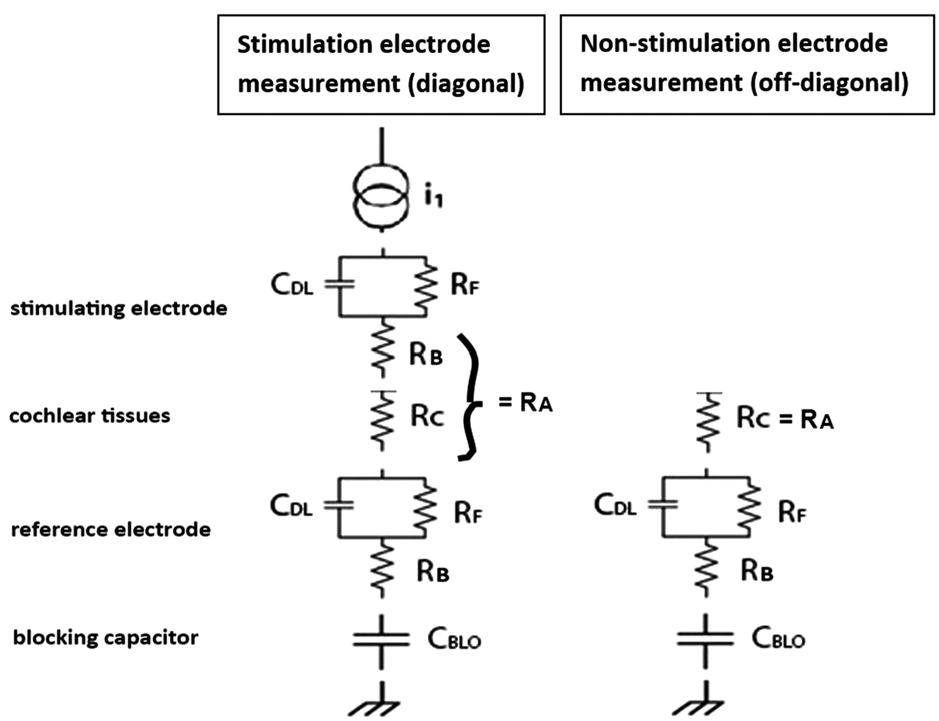

Figure 4. A model for the measurement of the voltage responses between the stimulating and the reference electrodes measured at the stimulating (left panel) and the reference (right panel) electrodes.

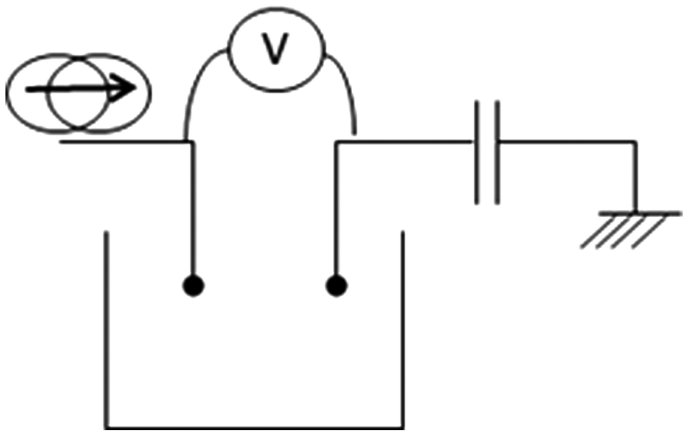

Figure 5. A model for the measurement of parameters constituting the impedance of the electrode–electrolyte interface.

be used. Any principally charge-balanced pulse type can be envisaged for use in the proposed approach, as long as the pulse does not cause charge transfer toward the tissue that might cause tissue damage.[13] The stimulating pulse can be a voltage or a current. One possible scheme of the measurement is shown in Figure 5.

A current pulse is injected at a stimulating electrode, and the voltage responses between the stimulating electrode and the reference electrode(s) are measured at the stimulating electrode (diagonal measurement) as well as between all other electrodes and the reference electrode(s) (off-diagonal measurements).[14] In the left-hand part of Figure 4, the relevant current signal path is illustrated for a diagonal measurement, i.e., a measurement at the stimulating electrode, and in the right-hand part for a nondiagonal measurement, i.e., at any of the nonstimulating contacts of the electrode array.

Voltage responses to the current pulses are recorded at different moments in time during the monopolar biphasic stimulation pulse. For example, a voltage response measurement may be performed for a biphasic pulse at, e.g., 10 instances as illustrated in Figure 6 (for a diagonal measurement on the left and a nondiagonal measurement on the right): at 6, 12, 18, 24, and 56 µs from the leading edge of each of the two pulse phases. In Figure 6, the left panel shows a typical voltage response measured at the stimulating electrode (diagonal measurement), while the right panel shows the voltage response measured at one of the nonstimulating electrodes of the electrode array (off-diagonal measurements). The dots are the measured data, whereas the solid line represents the model fitting of the signal received in response to the stimulation pulse.

The model parameters can be determined using the following approach: Essentially, the purely resistive component R_A contributes to the instantaneous response, i.e., the stepwise behavior of the waveform near the leading and trailing edges of the stimulation pulse, as can also be seen from Figure 6. For diagonal measurements, the parallel components R_F and C_{DL} result in an exponentially decaying/growing time response, as no current is assumed to flow through the electrode–tissue interface at electrodes different from the stimulation electrode. The Faradaic resistance R_F corresponds to the amplitude of the exponentially decaying/growing part of the response, whereas the double-layer capacitance C_{DL} is indirectly derived from the time constant τ ($\tau = C_{DL}\ R_F$). The implant-related blocking capacitance C_{BLO} gives rise to a linear slope with time during each phase of the stimulation pulse. The blocking capacitance C_{BLO} contributes to both the waveform measured at an electrode different from the intracochlear stimulation electrode (in a nondiagonal measurement) and the waveform at the stimulation electrode itself (in a diagonal measurement). Because C_{BLO} is common to the recordings at all intracochlear electrodes and because it is the only time-dependent contribution to the off-diagonal measurements, the linear effect of off-diagonal measurements is used to subtract the effect in the diagonal waveforms. This subtraction was already performed in the left panel of Figure 6. To exclude any effect of the stimulation current, C_{BLO} is preferably determined based on measurements obtained far away from the stimulation electrode. For example, measurements can be made at electrodes at least 18 electrodes away from the stimulating electrode in the array of electrodes.

The waveform fitting allows discriminating between the instantaneous resistive components and the time-dependent capacitive components of the impedance. However, the 2 resistive contributions R_B and R_C to the solution resistance R_A, seen when performing the diagonal measurements, cannot be separated, as the measurement procedure only yields their sum, $R_A = R_B + R_C$. To tackle this problem, it is assumed that the far-field component R_C, directly obtained for the waveforms away from the stimulation electrode, can be extrapolated toward the stimulation electrode. The far-field component R_C at the stimulation electrode is thus obtained by fitting the field

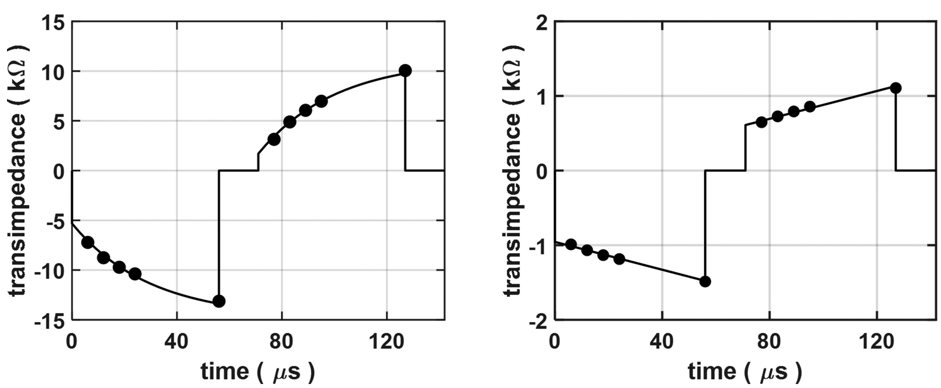

Figure 6. Voltage response measurement performed for a biphasic pulse at 10 time points at the stimulating electrode (left panel) and the nonstimulating electrode (right panel).

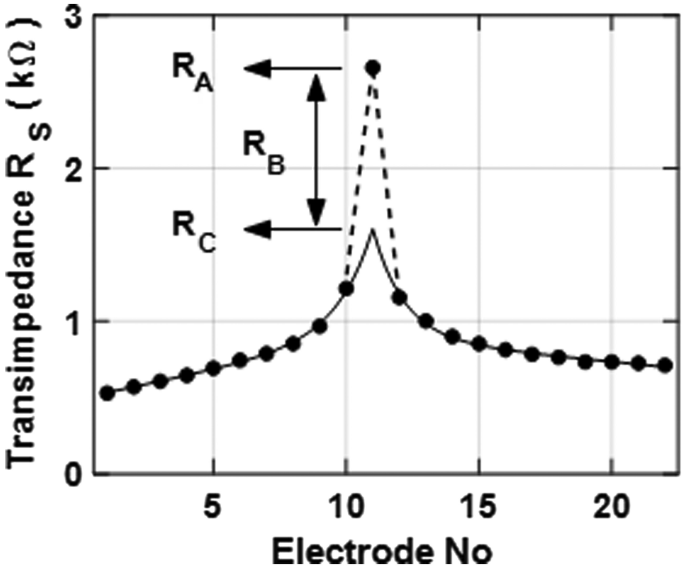

Figure 7. Extrapolation of the exponential decay of the nonstimulating electrode voltage amplitudes.

spread R_C from the nonstimulating measurements to a double-sided exponential on a linear function, with the constraint that basal and apical fitting meet each other at the stimulation electrode. Solution resistance R_A measured from the waveform fitting at the stimulation electrode diagonal measurement (Figure 6, left-hand panel) and R_C from extrapolating the nonstimulating field spread then also yield the bulk resistance R_B at the stimulation electrode. Figure 7 shows the extrapolation of the exponential decay of the off-diagonal (nonstimulating electrode) voltage amplitudes, allowing for the calculation of the R_C and the method for calculating the bulk resistance R_B at the stimulation electrode.

RESULTS

It was found that one particular component of the complex impedance model presented above very accurately correlates with the behavioral T/C levels, namely, the resistive component R_F corresponding to the Faradaic processes occurring at the electrode–electrolyte interface. This finding clearly indicates the importance of taking into account the near-field effects during simulations for fitting cochlear implants. The upper panel in Figure 8 shows the comparison of the correlations between the resistive R_F component and the behavioral T/C levels. The lower panel shows the same correlations for the overall impedance Z. The correlations for the R_F component ($R = -0.60$ for the T levels and $R = -0.73$ for the C levels) are much higher than for the overall impedance Z ($R = -0.40$ for the T levels and $R = -0.51$ for the C levels).

When we average the C level and R_F over the whole electrode array for each of the 18 patients, we notice even higher correlations with $R = -0.894$ (Figure 9).

For the majority of patients, it is sufficient to use only this resistive component, R_F, as a basis for prediction of the T/C levels in order to obtain satisfactory results. Figure 10 shows that the median result of the estimation of the T/C fitting parameters (measured behaviorally) over the various electrodes of the array in a number of patients indeed almost exactly agrees with the T/C levels calculated on the basis of the correlation with the resistive Faradaic component R_F. The upper curves in Figure 10 shows the differences found for the C levels and the lower curves for the T levels.

Although in most cases the agreement between the behaviorally measured T/C levels and the predictions calculated on the basis of the resistive component R_F alone is excellent, in some cases the standard

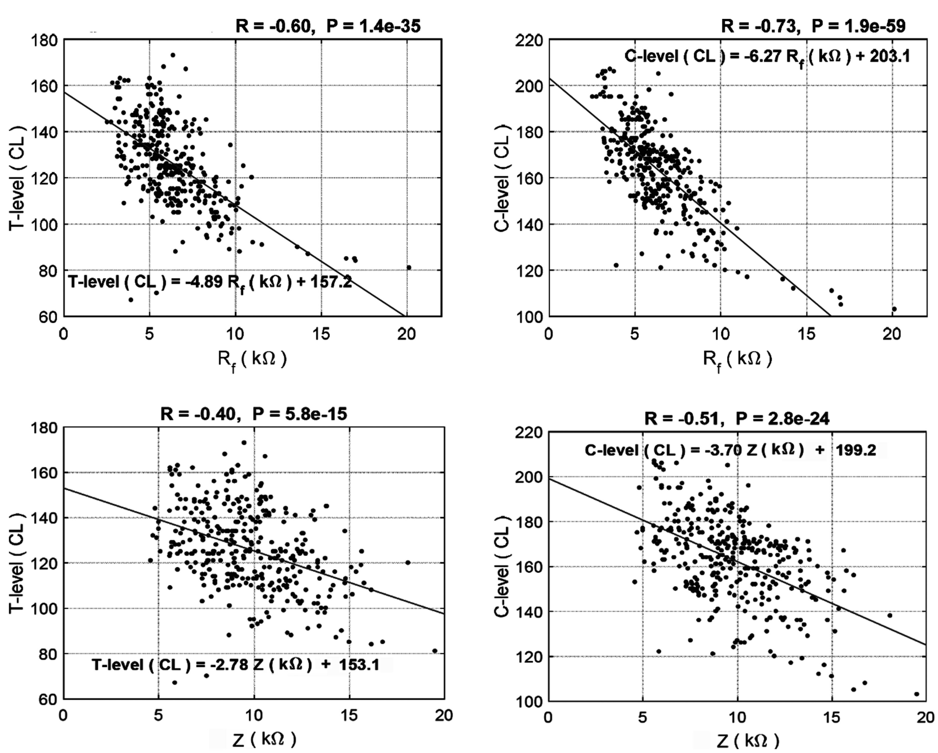

Figure 8. Comparison of the correlations between the resistive R_F component with the behavioral T/C levels (upper panel) and the same correlations for the overall impedance Z (lower panel).

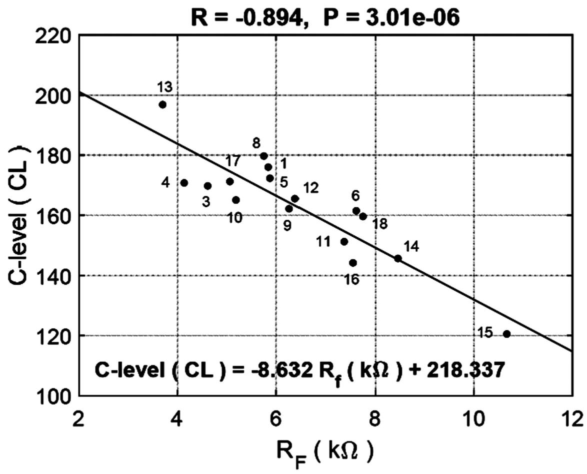

Figure 9. C level vs. R_F, where C level and R_F are averaged over the whole electrode array for each of the 18 patients.

deviation σ of the differences calculated for individual contacts is still large, as illustrated in Figure 11. The upper curve shows the standard deviation for the C levels and the lower curve for the T levels. Hence, in order to decrease the variability of the differences between the behaviorally measured T/C levels and the predictions calculated on the basis of the resistive component, additional parameters have to be added to the metric equation, allowing for automatic prediction of the T/C levels. These parameters will be described in separate publications.

DISCUSSION

Our recently published papers[5,15] show major improvements in the prediction of the behavioral T/C levels by analysis of the impedances of the electrode contacts compared to the methods based on the thresholds of evoked neural potentials (ECAP, EABR) or based on the thresholds of the electrically evoked stapedius muscle reflexes (ESRT). The impedances of the electrode contacts show significant strong negative correlations with the stabilized T/C levels at 4-6 months after implantation and are an important predictor for the behavioral T/C levels, especially for perimodiolar electrodes.[15] In these electrodes, the electrode impedances can explain 28%-41% (R^2) of the variability of the behavioral T/C levels.

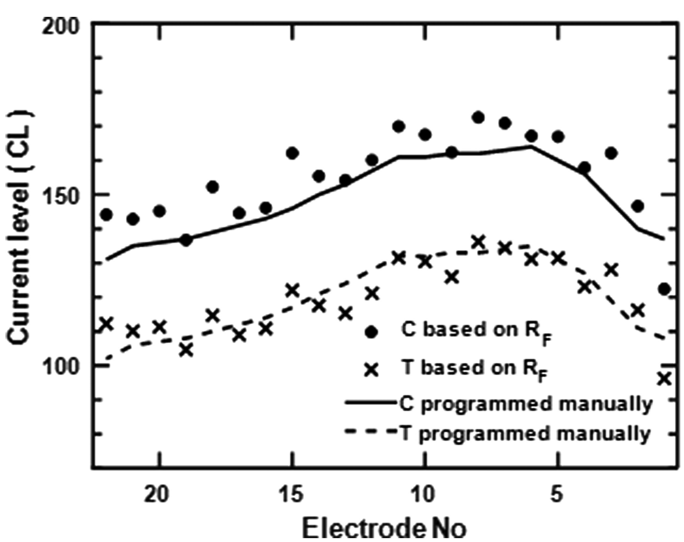

Figure 10. Comparison between the T/C levels based on R_F and programmed manually.

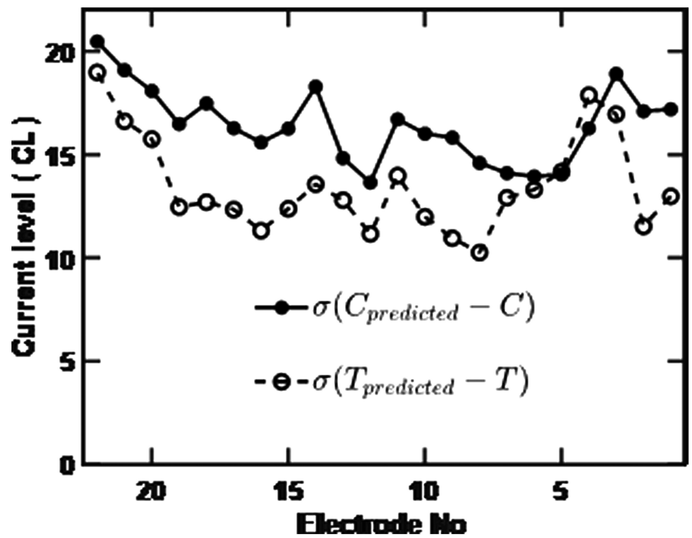

Figure 11. Standard deviation σ of the differences calculated for individual contacts in C levels (upper curve) and T levels (lower curve).

The method of calculating R_F presented above correlates even better than the overall compound impedance with the behavioral T/C levels and explains 80% (R^2) of the variability of the behavioral T/C levels. This allows for much better prediction of the T/C levels than based on the overall compound impedance Z.

As mentioned earlier, R_F is related to the electrochemical processes in the closest vicinity of the electrode contact (near-field effects).[6] The difference in the strength of correlation between the R_F values and the overall compound impedances strongly underlines the role of the near-field effects of the electrical stimulation and implies that the other elements of the compound impedance play a confounding role and decrease the correlation strength. From the electrical point of view, nerve fibers can be considered as a voltage-regulated current gate. Therefore, the higher the R_F values, the larger the voltage differences generated across the R_F and the higher the chance of eliciting an action potential in the neighboring nerve fibers. This explains why a negative correlation exists between the R_F value and the response thresholds.

Since these are the near-field effects that are most important for electrical stimulation of the neural tissues, it becomes more and more important to place the stimulating electrodes in the closest possible vicinity to the neural tissues.[16,17] In this optics, the perimodiolar cochlear implant electrodes should work better and show lower variability in the stimulation parameters. This has already been empirically observed by us in a previous study.[4]

This also explains why little electrophysiological and psychoacoustic differences are noticed when the current pathways are changed, by for example changing the position of the reference electrodes. The changes in the current pathways are unimportant because the near-field effects are decisive for the generation of action potentials in the nerve fibers. Due to the primary role of the near-field effects, the current spreads within the fluid spaces of the scala tympani and does not destroy the selectivity of stimulation with cochlear implant electrodes, and frequency-specific information can be delivered to well-defined areas of the cochlea.

However, in some patients, the predictions of the behavioral T/C levels based on calculation of the R_F value are not accurate, and the standard deviation σ of the differences between the predicted and measured T/C levels for individual contacts is still large (Figure 11). This explains why higher correlations are observed when the C level and R_F are averaged over the whole electrode array for each of the 18 patients (Figure 9).

Worse accuracy of predictions in some patients is due to the fact that the behavioral T/C levels depend not only on the voltages generated in the close vicinity of the neural tissues but also on the neural preservation and functionality as well as on the cognitive parameters defining the reaction of the auditory cortex to the patterns of electrical firing in the auditory nerves.[18,19] Therefore, in order to decrease the variability of the differences between the behaviorally measured T/C levels and the predictions calculated on the basis of the R_F value, additional parameters have to be added to the metric equation, allowing for automatic prediction of the T/C levels. These parameters will be described in separate publications.

A new method for deriving information from the electrode impedance measurements shows excellent correlation of the Faradaic resistance RF with the behavioral T/C levels in most patients and can be very useful for fitting cochlear implants based on objective measures. Since some patients still show discrepancies between the predicted T/C levels based on the R_F calculation, additional parameters have to be added to the metric equation to allow for automated prediction of the T/C levels.

Ethics Committee Approval: This study was running under the Ethics Committee approval of CTC5585 'Innovation in Clinical Care for Users of a Nucleus Cochlear Implant', obtained from the Ethics Committee of Sint Augustinus Hospital - Gasthuis Zusters Antwerpen (GZA) (Approval No: CTC5585, Date: January 9, 2015).

Informed Consent: Written informed consent was obtained from the patients who agreed to take part in the study.

Peer-review: Externally peer-reviewed.

Author Contributions: Concept – A.Z., M.L.; Design – A.Z., M.L., A.M.; Supervision – A.Z., M.L.; Resources – A.Z., J.v.D., F.E.O.; Materials – A.Z., M.L., A.M., F.S., J.v.D., F.E.O.; Data Collection and/or Processing – A.Z., M.L., A.M., F.S.; Analysis and/or Interpretation – A.Z., M.L., A.M., F.S.; Literature Search – A.M., F.S., J.v.D.; Writing – A.Z., M.L., A.M.; Critical Review – A.Z., M.L., A.M., F.S., J.v.D., F.E.O.

Declaration of Interests: The authors have no conflict of interest to declare.

Funding: The authors declared that this study has received no financial support.

REFERENCES

1. Molisz A, Zarowski A, Vermeiren A, et al. Postimplantation changes of electrophysiological parameters in patients with cochlear implants. *Audiol Neurootol*. 2015;20(4):222-228. [CrossRef]
2. Hughes ML, Vander Werff KRV, Brown CJ, et al. A longitudinal study of electrode impedance, the electrically evoked compound action potential, and behavioral measures in Nucleus 24 cochlear implant users. *Ear Hear*. 2001;22(6):471-486. [CrossRef]
3. Pourjavid A, Adel Ghahraman M, Sedaie M, Emamjome HA, Mobedshahi F, Abbasalipour Kabirrah P. Amplitude changes of the electrically evoked compound action potential in children with cochlear implants: preliminary results. *Iran J Pediatr*. 2011;21(3):390-394.
4. Zarowski A, Molisz A, Mylanus EAM, et al. Comparison of electrophysiological parameters between perimodiolar and lateral wall electrodes in paediatric cochlear implant users. *Eur Arch Otorhinolaryngol*. 2020; 277(10):2693-2699. [CrossRef]
5. Zarowski A, Molisz A, Cardinael E, et al. Prediction of behavioral T/C levels in cochlear implant patients based upon analysis of electrode impedances. *J Am Acad Audiol*. 2020;31(9):674-679. [CrossRef]
6. Newbold C, Mergen S, Richardson R, et al. Impedance changes in chronically implanted and stimulated cochlear implant electrodes. *Cochlear Implants Int*. 2014;15(4):191-199. [CrossRef]
7. Dymond AM. Characteristics of the metal-tissue interface of stimulation electrodes. *IEEE Trans Bio Med Eng*. 1976;(23)4:274-280. [CrossRef]
8. Lasia A. Electrochemical impedance spectroscopy and its applications. In: *Modern Aspects of Electrochemistry*. Kluwer Academic Publishers. 2002:143-248. [CrossRef]
9. Bard AJ, Faulkner LR. *Electrochemical methods : fundamentals and applications*. Chichester, UK: Wiley; 2001. Accessed December 4, 2019. https://www.wiley.com/en-be/Electrochemical+Methods:+Fundamentals+and+Applications,+2nd+Edition-p-9780471043720
10. Sue A, Tran P, Wong P, Li Q, Carter P. Time-domain finite element models of electrochemistry in intracochlear electrodes. In 2013 35th Annual International Conference of the IEEE Engineering in Medicine and Biology Society (EMBC). IEEE. 2013;2013:1554-1557. [CrossRef]
11. Kawano A, Seldon HL, Clark GM, Ramsden RT, Raine CH. Intracochlear factors contributing to psychophysical percepts following cochlear implantation. *Acta Otolaryngol*. 1998;118(3):313-326. [CrossRef]
12. Malherbe TK, Hanekom T, Hanekom JJ. The effect of the resistive properties of bone on neural excitation and electric fields in cochlear implant models. *Hear Res*. 2015;327:126-135. [CrossRef]
13. Harris AR, Newbold C, Carter P, Cowan R, Wallace GG. Using chronopotentiometry to better characterize the charge injection mechanisms of platinum electrodes used in bionic devices. *Front Neurosci*. 2019;13:380. [CrossRef]
14. Mesnildrey Q, Macherey O, Herzog P, Venail F. Impedance measures for a better understanding of the electrical stimulation of the inner ear. *J Neural Eng*. 2019;16(1):016023. [CrossRef]
15. Zarowski A, Molisz A, De Coninck L, et al. Influence of the pre- or post-lingual status of cochlear implant recipients on behavioural T/C-levels. *Int J Pediatr Otorhinolaryngol*. 2020;131:109867. [CrossRef]
16. Holden LK, Finley CC, Firszt JB, et al. Factors affecting open-set word recognition in adults with cochlear implants. *Ear Hear*. 2013;34(3): 342-360. [CrossRef]
17. Lee JY, Hong SH, Moon IJ, et al. Effect of cochlear implant electrode array design on electrophysiological and psychophysical measures: lateral wall versus perimodiolar types. *J Audiol Otol*. 2019;23(3):145-152. [CrossRef]
18. Kurz A, Grubenbecher M, Rak K, Hagen R, Kühn H. The impact of etiology and duration of deafness on speech perception outcomes in SSD patients. *Eur Arch Otorhinolaryngol*. 2019;276(12):3317-3325. [CrossRef]
19. Favaretto N, Marioni G, Brotto D, et al. Cochlear implant outcomes in the elderly: a uni- and multivariate analyses of prognostic factors. *Eur Arch Otorhinolaryngol*. 2019;276(11):3089-3094. [CrossRef]